

# Design and fabrication of a diaphragm type thermo-buckled microactuators

Jiun-Min Wang<sup>1\*</sup>, Hung-Hua Lin<sup>1</sup>, Yue-Jheng Lin<sup>1</sup>, Yu-Cheng Ou<sup>1</sup>,  
Lung-Jieh Yang<sup>1</sup>, Chii-Wann Lin<sup>2</sup>, Yao-Joe Yang<sup>3</sup> and Wei-Chih Lin<sup>4</sup>

<sup>1</sup> Department of Mechanical and Eelectro-mechanical Engineering, Tamkang University,  
No.151, Ying-Chuan Rd., Tamsui, 25137, Taiwan

<sup>2</sup> Institute of Biomedical Engineering, National Taiwan University, No.1, Sec.4, Roosevelt Rd., Taipei, 106, Taiwan

<sup>3</sup> Department of Mechanical Engineering, National Taiwan University, No.1, Sec.4, Roosevelt Rd., Taipei, 106, Taiwan

<sup>4</sup> Energy Resources Laboratories, ITRI, No. 195, Chung Hsing Rd., Sec.4, Chu Tung, Hsin Chu, 310, Taiwan

**Abstract**—This study presents a novel diaphragm type thermo-buckled microactuator with only a driving voltage of 3V and under a working temperature far below 100°C. It's a sandwich structure composed of a platinum (Pt) resistor between two parylene films with different thickness. The platinum resistor is assigned as a heating source. Therefore, the parylene diaphragm with different thicknesses of top and bottom layers is heated by the embedded Pt resistor. The non-uniform temperature rise of the parylene diaphragm not only generates an out-of-plane thermo-buckling deformation, but also induces an asymmetric deflection inclined to upward or downward direction. The maximum displacement of the diaphragm is 0.4  $\mu\text{m}$  and the cut-off frequency is 1000 Hz by a driving voltage of 3V.

**Keywords**—thermo-buckled; microactuator; parylene

## I. INTRODUCTION

Microactuators are widely used components in active MEMS devices. There are various driving approaches using magnetic, thermal, electrostatic, and piezoelectric principles. Among these working devices, thermal microactuators can generate large force, operate bi-directionally and require low operating voltage with simpler geometry design. Many researches involved with the in-plane microactuators, e.g., Guckel et al. [1] first fabricated a thermo-magnetic metal flexure actuator by LIGA. Fang et al. [2] developed the thermal actuators with out-of-plane motion and demonstrated the bi-directional actuation capability with a poly-MEMS process. However, the previous works used metals or polysilicon as the actuation materials, which must be heated up to 600°C or even higher temperature to obtain sufficient thermal stress for buckling. Such a working temperature of thermal actuators is too high to be applied to biological fields.

Recently, parylene thermal actuators were reported to be functioned well at low temperature [3] and demonstrated the ability of capturing micro bio-entities such as fish eggs [4]. Parylene has excellently thermal and electrical insulation properties and has a larger coefficient of thermal expansion than typical metals over one order of magnitude. The characteristic of large thermal expansion of parylene denotes that the working temperature can be reduced to 40-60°C, almost one order of magnitude lower than the working temperatures of polysilicon or metal thermal actuators.

Furthermore, there are other advantages of biocompatibility and low power consumption for parylene thermal actuators.

## II. DEVICES DESIGN

The 3D viewgraph of diaphragm type thermo-buckled microactuator is shown in Fig. 1. The diaphragm is a sandwich structure with a platinum resistor between two different thickness parylene films. The diaphragm actuation is due to the two parylene films heated by the platinum resistor and their different temperature rises. Finally, the diaphragm will be move out-of-plane by the thermo-buckling mechanism.

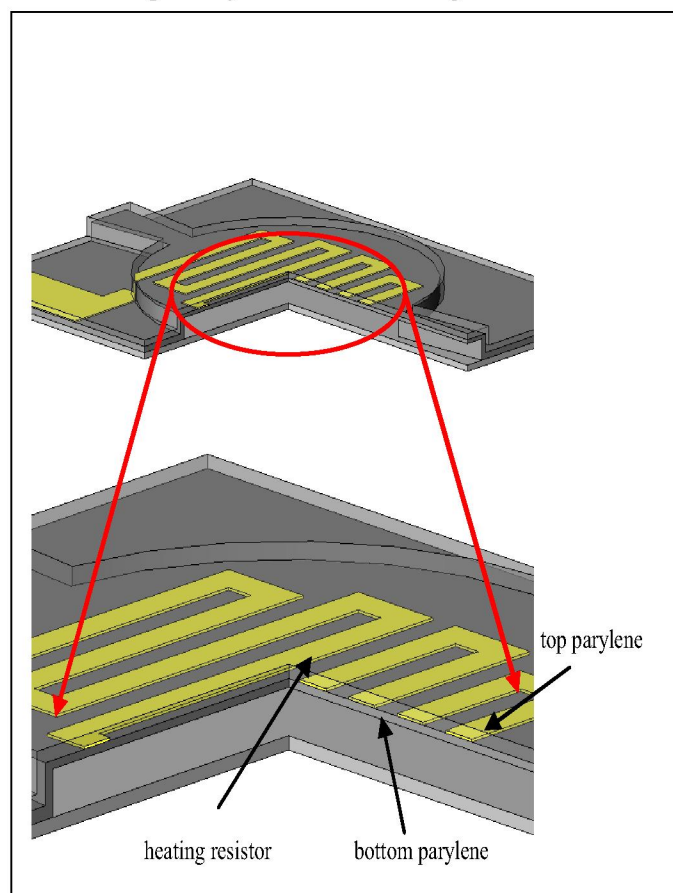


Fig. 1: 3D viewgraph of a diaphragm type thermo-buckled microatuator.

This work is supported by the project of Wireless Health Advance Monitoring Bio-Diagnosis System (WHAM-BioS), Ministry of Economic Affairs, Taiwan, with the project number of 94-EC-17-A-05-SI-017.

\*Contact author: 892340042@s92.tku.edu.tw

Before fabrication, we used the simplified bridge model to calculate the out-of-plane deflection of parylene thermal actuators at first. The maximum deflection of a simplified bridge model is [5]

$$d_0 = \pm a_0 l_0 \quad (1)$$

where  $l_0$  is the length of the bridge and  $a_0$  is defined in Eq. (2)

$$a_0 = \pm \frac{2}{\pi} \sqrt{\varepsilon - \left(\frac{\pi^2}{3}\right) t^2} \quad (2)$$

where  $\varepsilon$  is the strain of bridge and  $t$  is the ration of thickness to length of bridge. The strain is induced by the thermal stress and defined in Eq. (3)

$$\varepsilon = \frac{\sigma}{E} + \alpha \Delta T \quad (3)$$

where  $\sigma$  is the thermal stress,  $E$  is the Young's modulus (3.2GPa for parylene) ,  $\alpha$  is the thermal expansion coefficient ( $3.01 \times 10^{-5} \text{ } ^\circ\text{C}^{-1}$  for parylene) and  $\Delta T$  is the temperature difference between two parylene films. Because of this study diaphragm composed of two parylene films, the thermal stress can be represented in Eq. (4)

$$\sigma = \frac{\sigma_1 t_1 + \sigma_2 t_2}{t_1 + t_2} \quad (4)$$

where  $\sigma$  and  $t$  are thermal stress and thickness of parylene films. The index 1 represents the bottom parylene and the index 2 indicats the top parylene.

We assumed the temperature difference between top and bottom parylene is 40 degree C and the thicknesses of two parylene are 1 $\mu\text{m}$  and 2 $\mu\text{m}$ , respectively. The computing maximum deflection of parylene simplified bridge model by Eq. (1) ~ Eq. (4) is shown in table 1.

Table1: The maximum deflection of simplified bridge model with 40  $^\circ\text{C}$  temperature difference between two parylene films. (unit: $\mu\text{m}$ )

Length of bridge	200	300	400
Maximum deflection	2.7	5.7	8.1

Beside, This study also accessed finite element analysis ANSYS to preliminarily confirm the design prediction. The element we used in ANSYS is the electro-thermal-stress coupled element. It is closer to real displacement of the actuator and better than the deflection predicted by the simplified bridge model. Table 2 summarized the simulation deflection caused by the thermal buckling of the diaphragm type parylene actuator with 300  $\mu\text{m}$  diameter, and Fig. 2 shows the result of ANSYS simulation.

Table 2: The deflection caused by the thermal buckling of the diaphragm type parylene actuator with 300  $\mu\text{m}$  diameter;  $t_1$  and  $t_2$  are the bottom and top parylene film thickness (unit:  $\mu\text{m}$ .)

Design no.	#1	#2	#3	#4
$t_1$	0.3	0.5	1	1.5
$t_2$	0.6	1	2	3
Maximum displacement	1.93	1.83	1.03	0.66

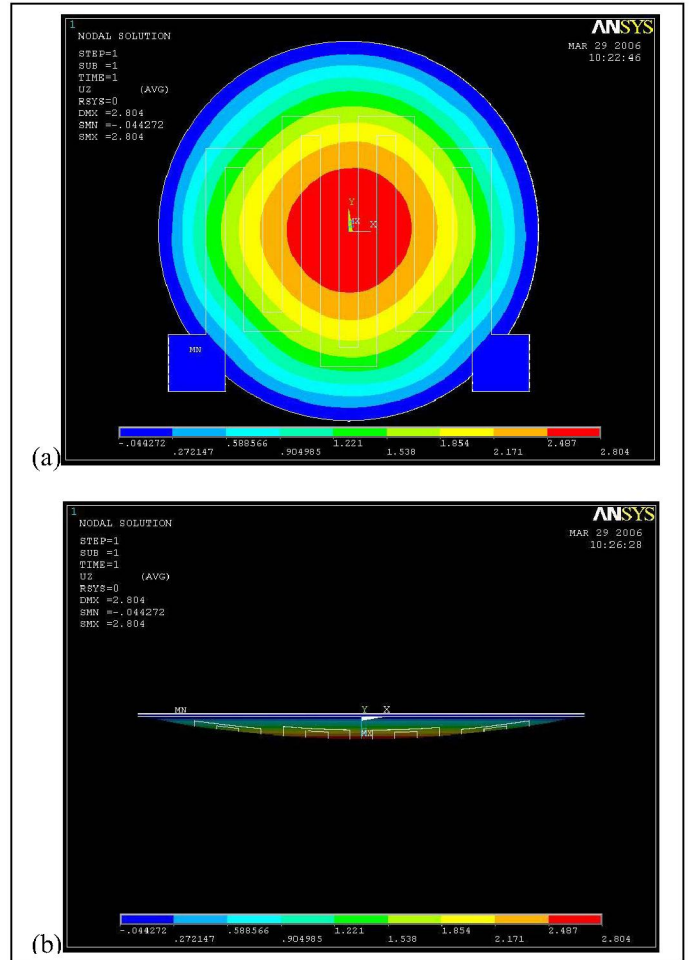


Fig. 2: Results of ANSYS simulation; (a) top view; (b) cross- section view



### III. DEVICES FABRICATION

We define the height of the pumping chamber by the thickness of photoresist sacrificial layer. We also choose  $t_1$  to be  $0.5\mu\text{m}$ , and  $t_2$  to be  $1\mu\text{m}$ , respectively (the total thickness of the parylene diaphragm is  $1.5\mu\text{m}$ ). The processing sequence of the new microactuator is depicted in Fig.3:

- 1) Deposit  $1\mu\text{m}$  thick parylene as a buffer base on a silicon substrate grown with oxide, and define the positions of input/output (I/O) pads.
- 2) AZ4620 photoresist is assigned and patterned as the sacrificial layer.
- 3) The lower or bottom parylene layer is deposited the same procedure as step (1).
- 4) Use lift-off technique to pattern the Pt resistor and I/O pads.
- 5) The top parylene is deposited conformally, and defined with the etching windows for dissolving sacrificial layer later on.
- 6) The sacrificial layer is dissolved by acetone finally. The completed device is shown in Fig. 4(a).

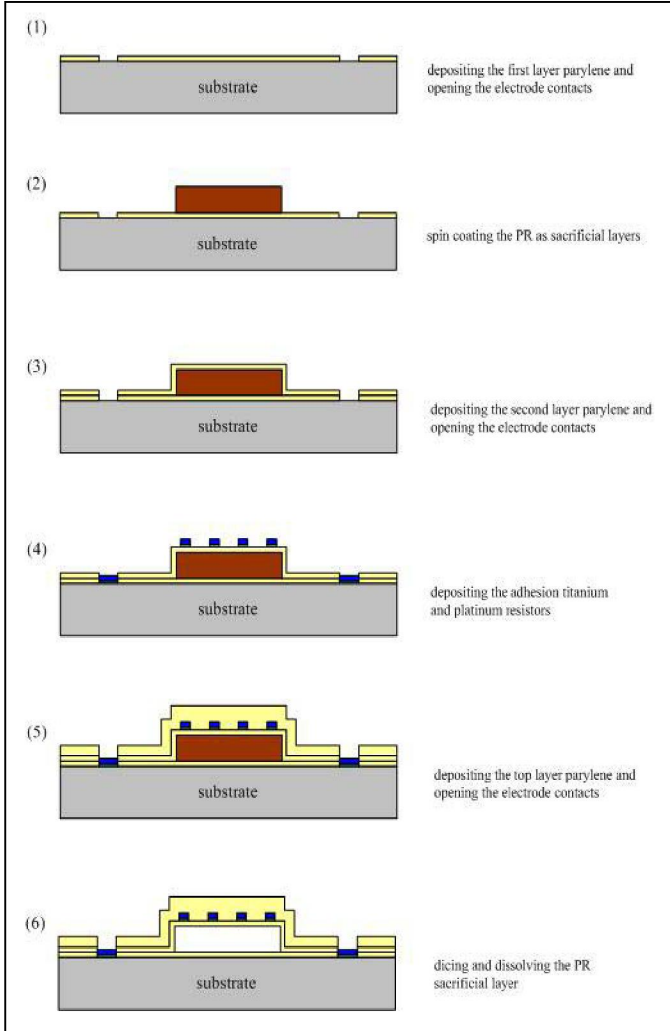


Fig. 3: Processing sequence of the new microactuator

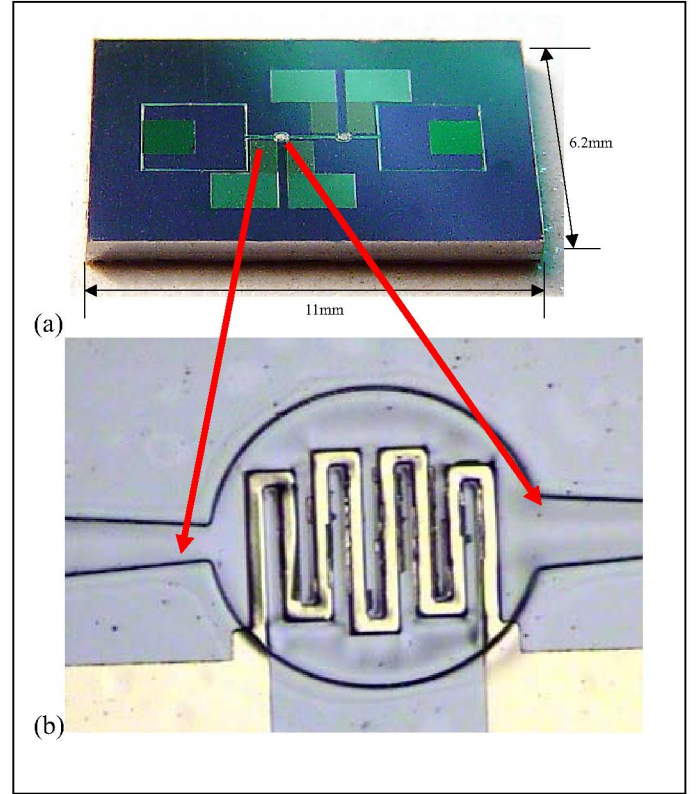


Fig 4: Completed parylene microactuator device; (a) the dimension of a whole chip; (b) the parylene diaphragm ( $300\mu\text{m}$ ) during operation.

### IV. RESULTS AND DISCUSSIONS

To verify the dynamic behavior of the completed thermo-buckled microactuator, we used an optical interferometer (*AVID<sup>TM</sup>*) to monitor the actuating vibration amplitude. The parylene diaphragm during operation is shown as Fig. 4(b). The peak-to-peak voltage of a driving square-wave is 3V and the frequency ranges from 1 Hz to 7,000 Hz. One time-varying deformation signal picked by the interferometer during device operation is shown in Fig. 5. The maximum deformation (subject to 5Hz square-wave) is only  $0.35\mu\text{m}$ , much smaller than the theoretical value of a static buckling. This can be explained by the excuse that the genuine heating or temperature distribution over the whole parylene actuation diaphragm is not really uniform, in other words, not like the case of simulation results in Fig. 2 and table 2. Another reason is that the simulation model is ideally a disk, not like the real geometry in Fig. 1.

Finally, the frequency response of a fabricated parylene actuator is experimentally investigated and sketched in Fig. 6. The dynamic result shows that the cut-off frequency is about 1000 Hz, much smaller than the first natural frequency (54,000 Hz; based on the assumption that parylene is an elastic material with Young's modulus of 3.2 GPa) of the parylene diaphragm. There's also no resonance response observed from Fig. 6, denoting that the fluidic squeezing is apparent and acts like a damper in a dynamic system.

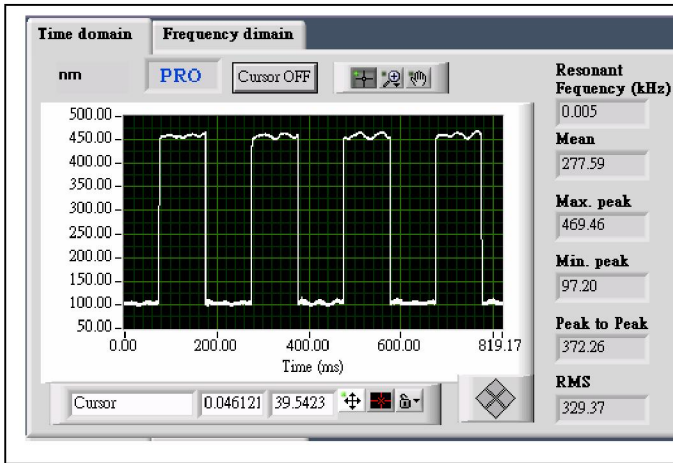


Fig. 5: Time-varying deformation signal picked by *AVID<sup>TM</sup>* optical interferometer during device operation (the diameter of diaphragm is 300 $\mu$ m.)

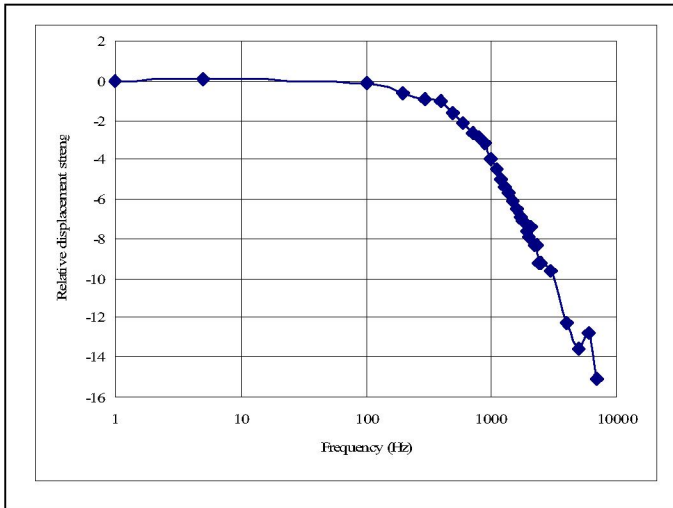


Fig. 6: Frequency response of a fabricated parylene actuator (the diameter of diaphragm is 300 $\mu$ m ); the relative displacement strength is defined as  $20 \log(d_f / d_1)$ ; where  $d_f$ ,  $d_1$  denote the maximum deflection subject to the vibrating frequency and 1 Hz respectively

## V. CONCLUSION

Restated, we novelly demonstrated a parylene thermal actuator of sub-mm size driven by a low voltage without apparent temperature rise. Such an extremely small and low-temperature device can be hopefully integrated and applied into biologically fluidic systems like valveless pumps [6-8].

## ACKNOWLEDGMENT

We would like to thank Dr Chih-Feng Lin of Tamkang University for his help in ANSYS. This work is supported by the project of Wireless Health Advance Monitoring Bio-Diagnosis System (WHAM-BioS), Ministry of Economic Affairs, Taiwan, with the project number of 94-EC-17-A-05-SI-017.

## REFERENCES

- [1] H. Guckel, J. Klein, T. Christenson and K. Skrobis, "Thermo-Magnetic Metal Flexure Actuators," Proc. Transducers'92, pp.73-75.
- [2] Wen-Chih Chen, Jerwei Hsieh and Weileun Fang, "A Novel Single-layer Bi-directional Out-of-plane Electrothermal Microactuator," Proc. MEMS 2002, pp.693-697, or Sensors and Actuators A, vol. 103, pp. 48-58, 2003.
- [3] J. W. L. Zhou, H. Y. Chan, T. K. H. To, K. W. C. Lai and W. J. Li, "Polymer MEMS actuators for underwater micromanipulation" Transactions on Mechatronics, vol. 9, Issue 2, pp. 334-342, 2004.
- [4] H. Y. Chan and W. J. Li, "Design and Fabrication of A Micro Thermal Actuator for Cellular Grasping" Acta Mechanica Sinica/Lixue Xuebao, vol. 20, Issue 2, pp.132-139, 2004.
- [5] T. Seki, M. Sakata, T. Nakajima and M. Matsumoto, "Thermal Buckling Actuator for Micro Relays," Proc. Transducers'97, pp.1153-1156.
- [6] E. Stemme and G. Stemme, "A Valveless Diffuser/Nozzle-based Fluid Pumps," Sensors and Actuators A, vol. 39, pp. 159-167, 1993.
- [7] A. Olsson, G. Stemme and E. Stemme, "A Valve-less Planar Fluid Pump With 2 Pump Chambers," Sensors and Actuators A, vol. 47, pp. 549-556, 1995.
- [8] A. Olsson, P. Enoksson, G. Stemme and E. Stemme, "A Valve-less Planar Pump Isotropically Etched in Silicon," Journal of Micromechanical and Microengineering, vol. 6, pp. 87-91, 1996.